Time-domain simulation and spectrum measurement of low-noise oscillators

Rémi Brendel, and Enrico Rubiola
FEMTO-ST Institute, Time and Frequency Dept.
CNRS, ENSMM, and UF-C, UMR 6174
Besançon, France
brendel@femto-st.fr and rubiola@femto-st.fr

***Abstract*—This paper deals with the modeling of noise spectra in high Q–factor oscillators so as to better understand the noise mechanism and to improve the low noise oscillator design. The dipolar method used is first demonstrated on a simple behavioral oscillator. Noise analysis consists in calculating the steady state and the transient response in the vicinity of the steady state with asymptotic methods. Then, the oscillator noise is calculated by introducing a small sinusoidal perturbation to the steady state. This allows to analyze both additive and parametric noise. The model provides time-domain waveforms, AM and PM noise spectra, and analytically explains the Leeson model.**

I. INTRODUCTION

In the past decades a large amount of work and effort has been spent in understanding the origin of the phase noise, in analyzing its influence on the oscillator stability, and in improving the oscillator design. In the meanwhile, the demand of low phase noise for space, communication and radar systems is ever and ever increasing. Emerging technologies, however promising, still have no viable alternatives to the quartz resonator. Thus, further theoretical and experimental investigations are necessary, aimed at understanding better the resonator, the oscillator loop, the simulation techniques, and the instruments. In most quartz oscillators the sustaining amplifier is a transconductance amplifier, implemented as a negative-real-part impedance connected in parallel to the resonator.

The standard numerical simulation tools, like SPICE, turn out to be unsuitable to the direct analysis of the oscillator because the oscillator is determined by a large-ratio pair of time constants, the period T and the relaxation time $\tau = QT/\pi$. The ratio τ / T is up to 1.5 10^6. In this condition, the simulation fails because of round-off errors and convergence problems.

II. DIPOLAR METHOD

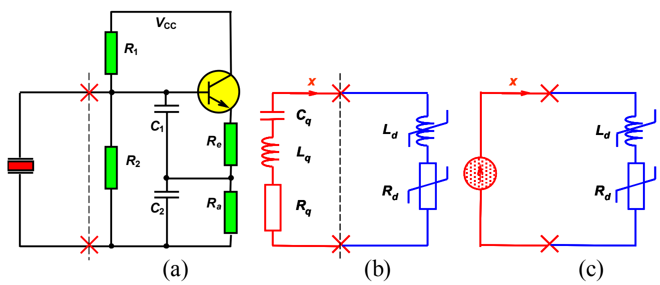

Figure 1. Simple Colpitts oscillator and dipolar modeling.

As shown in Fig. 1, an oscillator can be thought of as an association between a resonator whose impedance is strongly varying with frequency but weakly varying with the current amplitude and a sustaining active dipole whose impedance strongly vary with the current amplitude but weakly vary with the frequency [1]–[3].

Direct analysis of the whole circuit is often difficult because of the very high time constant introduced by the resonator branch. Thus, to overcome this issue, the circuit is split into two parts characterized independently.

Because of the high selectivity of the resonator series branch, it can be considered as a quasi-perfect sinusoidal source whose frequency is close to the resonant frequency. On the other side, in the vicinity of the resonant frequency, the amplifier dipole can be considered as a series combination of a resistance and a reactance which are nonlinear function of the current amplitude and can be characterized by replacing the resonator series-branch by a sinusoidal current source.

By giving the current source amplitude larger and larger values, it is possible to calculate the dipolar impedance as a function of the current amplitude and the curves obtained look as shown in Fig. 2.

This work is partly supported by the Centre National d'Études Spatiales (*French National Space Agency*).

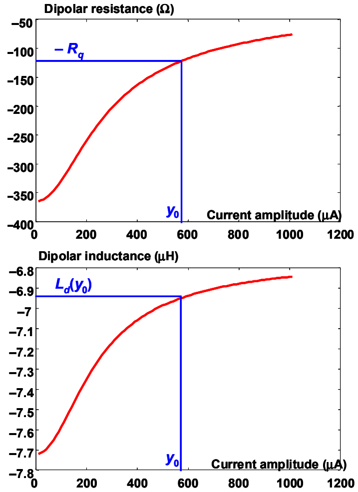

Figure 2. Dipolar impedance of a Colpitts oscillator.

When the resonator is connected to the dipolar impedance, the steady state oscillation condition is quite simple: the sum of the two impedances is null: $Z_q + Z_d = 0$ meaning that the two resistances and the two reactances have each equal and opposite values and this occurs for only one amplitude and one frequency. The amplitude is the current for which the dipolar resistance cancels the series branch resistance of the resonator: $R_d(y_0) = -R_q$, and the corresponding reactance value is straight related to the oscillation frequency:

$$\omega_0 = \omega_q \left(1 - \frac{L_d(y_0)}{2L_q} \right). \quad (1)$$

III. BEHAVIOURAL TRANSCONDUCTANCE OSCILLATOR

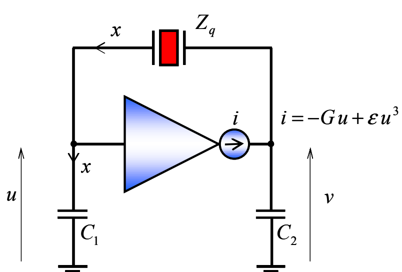

Figure 3. Behavioral transconductance oscillator.

The dipolar analysis can be demonstrated on the simple example shown in Fig. 3 which is a Colpitts-like circuit [3]. The sustaining amplifier is an ideal amplifier except it has a nonlinear cubic transconductance. This example is interesting because all features can be obtained by simple mathematics under analytical form. As previously described, the resonator is replaced by a sinusoidal current source of frequency ω_q: $x = y \sin \omega_q t$. By calculating the dipolar voltage and retaining only the fundamental component of its Fourier expansion, the dipolar impedance can be expressed as a function of the current amplitude y. In this particular case, the reactance is constant:

$$\begin{cases} \overline{R}_d = -Z_1 Z_2 \left(G - \dfrac{3\varepsilon Z_1^2 y^2}{4} \right) \\ \overline{X}_d = -(Z_1 + Z_2) \end{cases} \quad Z_1 = \frac{1}{\omega_q C_1} \quad Z_2 = \frac{1}{\omega_q C_2} \quad (2)$$

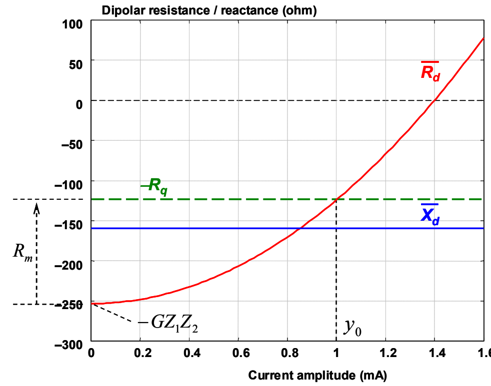

Figure 4. Dipolar impedance of the transconductance oscillator.

Fig. 4 shows that the dipolar resistance, which is a quadratic curve, is obviously negative at low amplitude, this condition being mandatory to insure the starting of oscillation.

Plotting on the same graph the opposite of the resonator resistance $-R_q$, evidences the oscillation current amplitude y_0 and the resistance margin R_m which characterizes the ability of the amplifier to start oscillations:

$$R_m = G Z_1 Z_2 - R_q \,. \quad (2)$$

The reactance of the amplifier plotted on the same graph gives the oscillation frequency expressed here as the frequency shift with respect to the quartz resonant frequency:

$$\frac{\Delta f}{f} = \frac{-\overline{X}_d(y_0)}{2L_q \omega_q}. \quad (3)$$

IV. NOISE SOURCES MODELING

Two main noise sources will be considered here: additive noise source such as thermal or shot noise, and parametric –mainly low frequency– perturbation coming for a large part from external influences. Most of the critical information concerning the noise sources can be obtained by replacing them with small independent sinusoidal sources and, according to the kind of perturbation, only considered in a small frequency range.

Because of the nonlinearity the effect of noise sources depends on their location, in particular, linear reduction of the noise sources to a single location may lead to wrong result.

Fig. 5 resumes the previous example with an additive noise source introduced in the amplifier input. Its magnitude is supposed very small with respect to the loop current amplitude: $\hat{x}_n << y$ and only a small frequency range close to the oscillation frequency will be considered:

$$\omega = \omega_q + \Omega \quad \Omega \gtrless 0 \quad |\Omega| << \omega_q \,. \quad (4)$$

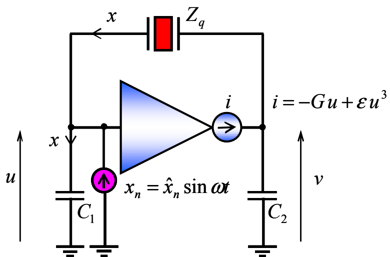

Figure 5. Transconductance oscillator with additive noise source.

Calculation of the dipolar impedance shows that it can be expressed under the following form:

$$\begin{cases} R_d = \overline{R}_d + \widetilde{R}_d \\ X_d = \overline{X}_d + \widetilde{X}_d \end{cases}, \tag{5}$$

where each component is the sum of two terms: the first part is the unperturbed impedance previously obtained and the alternating part depicts the perturbation effect which can be expressed under the following form:

$$\begin{cases} \widetilde{R}_d = R_{ds} \sin \Omega t + R_{dc} \cos \Omega t \\ \widetilde{X}_d = X_{ds} \sin \Omega t + X_{dc} \cos \Omega t \end{cases}, \tag{6}$$

where Ω represents the beat frequency between the perturbation source and the oscillation frequencies. The coefficient are shown here:

$$R_{ds} = \frac{\hat{x}_n Z_1}{y} \qquad R_{dc} = \frac{-\hat{x}_n Z_1 Z_2}{y}\left(G - \frac{9\varepsilon Z_1^2 y^2}{4}\right). \tag{7}$$
$$X_{ds} = \frac{-\hat{x}_n Z_1 Z_2}{y}\left(G - \frac{3\varepsilon Z_1^2 y^2}{4}\right) \qquad X_{ds} = \frac{-\hat{x}_n Z_1}{y}$$

Parametric noise source can be simulated by considering a sinusoidal low frequency modulation of the capacitor C_1 where the modulation index is very small and only low modulation frequencies are considered:

$$C_1 = \overline{C}_1(1 + \alpha \sin \Omega t) \qquad \alpha \ll 1 \qquad \Omega \ll \omega_q. \tag{8}$$

In this case, the dipolar impedance takes the same form as for the additive noise, only the expression of the coefficients is different:

$$\begin{Bmatrix} R_{ds} = \alpha Z_1 Z_2 \left(G - \frac{9\varepsilon Z_1^2 y^2}{4}\right) & R_{dc} = 0 \\ X_{ds} = \alpha Z_1 & X_{ds} = 0 \end{Bmatrix}. \tag{9}$$

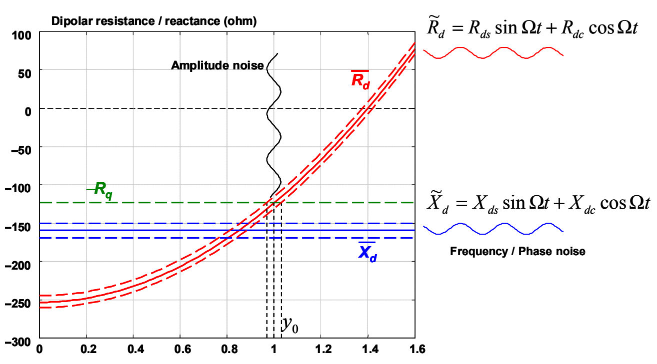

Figure 6. Dipolar impedance of a perturbed oscillator.

The dipolar method explains how noise sources affect both amplitude and frequency of the oscillation. Fig. 6 shows, in solid lines, the unperturbed dipolar impedance. The noise sources causes a low frequency change of the dipolar resistance, in dotted lines, and because of the equilibrium condition the amplitude is modulated at the same low frequency. Likewise, the noise induced reactance change produces a frequency modulation.

V. Noisy Oscillator Dipolar Analysis

Time-domain analytical calculation of the amplitude and frequency perturbation is possible by considering the oscillation loop shown in Fig. 1 (b). The two impedances facing each other are first expressed in the Laplace's form. The resonator series-branch impedance is given by:

$$Z_q = \frac{L_q}{s}\left(s^2 + \frac{R_q}{L_q}s + \omega_q^2\right) \tag{10}$$

and the dipolar impedance by:

$$Z_d = R_d + \frac{s}{\omega_q} X_d \tag{11}$$

where R_d and X_d are given by (5) and (6). The oscillation condition states that the two impedances have opposite values and this leads to the following equation:

$$\left(s^2 + \frac{R_q}{L_q}s + \omega_q^2\right)x = \frac{-1}{L_q}\left[s(R_d x) + s^2(L_d x)\right]. \tag{12}$$

Replacing the Laplace's operator by the differential operator leads to the following nonlinear and non-autonomous differential equation:

$$\begin{aligned} \ddot{x} + \omega_q^2 x = \frac{-1}{L_q}\left(R_q + \overline{R}_d\right)\dot{x} - \frac{\overline{X}_d}{L_q \omega_q}\ddot{x} \\ -\frac{1}{L_q}\left[\left(\dot{\widetilde{R}}_d + \frac{\ddot{\widetilde{X}}_d}{\omega_q}\right)x + \left(\widetilde{R}_d + \frac{2\dot{\widetilde{X}}_d}{\omega_q}\right)\dot{x} + \frac{\widetilde{X}_d}{\omega_q}\ddot{x}\right] \end{aligned}. \tag{13}$$

Without entering in the detail, we can see here that the right hand side term is composed of an autonomous nonlinear term and a slowly varying perturbation term due to the noise sources.

VI. Slowly Varying Function Method

The slowly varying function method, specially developed more than 60 years ago to solve asymptotically that kind of problem [4], consists in transforming the high frequency second order differential equation into a first order differential system in the slowly varying amplitude $y(t)$ and phase $\varphi(t)$ variables by using the variable change:

$$x = y(t)\cos(\omega_q + \varphi(t)) \tag{14}$$

that leads to the so-called *associated system*:

$$\begin{aligned} \dot{y} &= \frac{-y}{2L_q}\left(R_q + \overline{R}_d\right) - \frac{y}{2L_q}\left(A_s \sin \Omega t + A_c \cos \Omega t\right) \\ \dot{\varphi} &= \frac{-\overline{X}_d}{2L_q} + \frac{1}{2L_q}\left(B_s \sin \Omega t + B_c \cos \Omega t\right) \end{aligned}. \tag{15}$$

A_s, A_c, B_s, and B_c are time-constant coefficients that are function of the low frequency Ω and of the coefficients R_{ds}, R_{dc}, X_{ds}, and X_{dc} defined by (7) or (9). The associated system is composed of an autonomous part and a slowly time varying perturbation term due to the dipolar impedance modulation. Because of the smallness of the perturbation terms, their influence can be expressed by using a perturbation method around the oscillation steady state obtained by solving the unperturbed associated system:

$$\begin{aligned} \dot{y} &= \frac{-y}{2L_q}\left(R_q + \overline{R}_d\right) \\ \dot{\varphi} &= \frac{-\overline{X}_d}{2L_q} \end{aligned} . \qquad (16)$$

The steady state is reached when the amplitude becomes constant, i.e. when $\dot{y}=0$. This occurs for the steady state amplitude y_0 and the oscillation frequency ω_0 represented in Fig. 4 that are given by:

$$R_d(y_0) = -R_q \qquad \Rightarrow \qquad y_0^2 = \frac{4R_m}{3\varepsilon Z_1^3 Z_2}, \qquad (17)$$

$$\omega_0 = \omega_q + \nu_0 \qquad \nu_0 = \dot{\varphi}(y_0) = \frac{-X_d(y_0)}{2L_q}. \qquad (18)$$

Perturbation terms will only induce small changes around the steady state. They can be expressed under the form:

$$\begin{cases} y = y_0 + z & |z| << y_0 \\ \dot{\varphi} = \nu_0 + \eta & |\eta| << \omega_q \end{cases} . \qquad (19)$$

Retaining only first order terms, the linearized perturbation equations take the following form:

$$\begin{cases} \dot{z} + \Omega_R z = -\dfrac{y_0}{2L_q}\left(A_s \sin\Omega t + A_c \cos\Omega t\right) \\ \eta = \dfrac{1}{2L_q}\left(B_s \sin\Omega t + B_c \cos\Omega t\right) \end{cases} \qquad (20)$$

where:

$$\Omega_R = \frac{R_m}{L_q}, \qquad (21)$$

R_m being the resistance margin given by (2). The elementary linear system (20) has a sinusoidal solution of the form:

$$\begin{cases} z = \hat{z}\cos(\Omega t - \varphi_z) \\ \eta = \hat{\eta}\cos(\Omega t - \varphi_\eta) \end{cases} \qquad (22)$$

where φ_z and φ_η are some insignificant constant phase shifts.

System (22) expresses that a noise current source induces both AM and FM modulation of the loop current at frequency Ω. For additive noise, Ω is the beat frequency between excitation and oscillation frequencies while for low frequency parametric noise, Ω is merely the modulation frequency.

VII. AM and FM Lines and Noise Spectra

AM and FM line amplitudes are obtained by putting (22) in (20) and solving it for $\hat{z}$ and $\hat{\eta}$. Replacing in the result A_s, A_c, B_s, and B_c by their expression with the coefficients R_{ds}, R_{dc}, X_{ds}, and X_{dc} defined by (7) leads to the following result for the additive noise source:

$$\begin{cases} \hat{z} = \dfrac{\hat{x}_n}{2L_q} \dfrac{\sqrt{Z_1^2 + \left(3R_q - 2GZ_1Z_2\right)^2}}{\sqrt{\Omega_R^2 + \Omega^2}} \\ \hat{\eta} = \dfrac{\hat{x}_n}{2L_q y_0}\sqrt{Z_1^2 + R_q^2} \end{cases} . \qquad (23)$$

The same processes applied to parametric noise source leads to the following result:

$$\begin{cases} \hat{z} = \dfrac{\alpha\, y_0}{2L_q} \dfrac{\sqrt{\dfrac{4Z_1^2\Omega^2}{\omega_q^2} + \left(3R_q - 2GZ_1Z_2\right)^2}}{\sqrt{\Omega_R^2 + \Omega^2}} \\ \hat{\eta} = \dfrac{\alpha}{2L_q}\sqrt{Z_1^2 + \dfrac{\Omega^2}{\omega_q^2}\left(3R_q - 2GZ_1Z_2\right)^2} \end{cases} . \qquad (24)$$

The amplitude noise spectrum is nothing else than the variation of the AM line with respect to the modulation frequency, thus it takes the simple form:

$$S_z(\Omega) = 10\log\left(\frac{\hat{z}^2}{2y_0^2}\right), \qquad (25)$$

It is more usual to represent the phase noise spectrum rather than the frequency noise spectrum. Phase φ and frequency η are related by a linear transfer function so their spectra obey the classical relation:

$$\varphi = \frac{\eta}{j\omega} \qquad \Rightarrow \qquad S_\varphi(\omega) = \frac{1}{\omega^2} S_\eta(\omega), \qquad (26)$$

and the phase noise spectrum can be obtained from the FM line variation by the relation:

$$S_\varphi(\Omega) = 10\log\left(\frac{\hat{\eta}^2}{2\Omega^2}\right). \qquad (27)$$

VIII. Noise Spectra of the Loop Current

To illustrate the result previously obtained, let's consider the case of a white current source associated with a 50 Ω resistance, the amplitude of which is of the order of a few $\mathrm{pA}/\sqrt{\mathrm{Hz}}$.

As shown in Fig. 7, the phase noise spectrum of the loop current (solid line) is merely a straight line of slope –20 dB/decade, while the amplitude noise spectrum (dashed line) exhibits a resonance shape the half bandwidth of which is given by (21) where R_m given by (2) is related to the nonlinearity of the amplifier.

The cut-off frequency Ω_R of the amplitude modulation resonance allows us to define what can be considered as the oscillator closed loop Q-factor:

$$Q_R = \frac{\omega_q}{2\Omega_R} = \frac{\omega_q L_q}{R_m}, \qquad (28)$$

Q_R that can be greater or lower than the resonator unloaded Q-factor is straight related to the starting time of the oscillator.

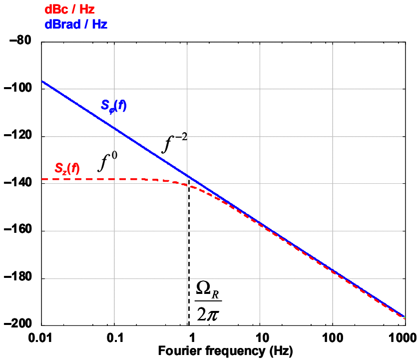

Figure 7. Additive noise amplitude and phase spectra of the loop current.

Let's consider now the case of a parametric noise source represented by a low frequency modulation of the input capacitor C_1. In addition, the modulation is supposed to have a $1/f$ spectrum with a floor modulation index $\alpha_0 = 10^{-8}$ and a corner frequency $\Omega_k/(2\pi) \approx 1$ Hz:

$$C_1 = \overline{C}_1\left(1 + \alpha \sin \Omega t\right) \qquad \alpha^2 = \alpha_0^2\left(1 + \frac{\Omega_k}{\Omega}\right) \tag{29}$$

In this case, the phase noise spectrum shown in Fig. 8 (solid line) exhibits a – 30dB/dec slope up to the corner frequency, beyond it recovers the usual –20 dB/dec slope.

The amplitude spectrum (dashed line), has a –10dB/dec slope within the bandwidth of the modulation resonance, followed by a –30 dB/dec up to the corner frequency and the usual –20dB/dec beyond the corner frequency. In the particular case shown in Fig. 8, the corner frequency coincides with the closed loop cut-off frequency.

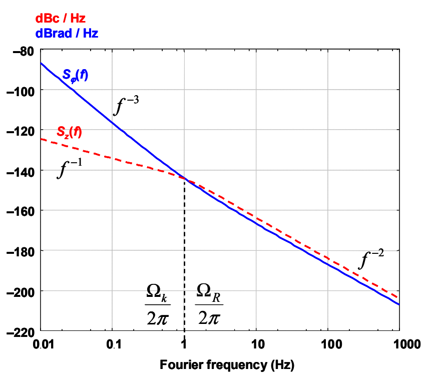

Figure 8. Parametric noise amplitude and phase spectra of the loop current.

IX. Oscillator Output Voltage

In any oscillator, the output signal is not the loop current but a voltage, and the noise spectra of the output voltage can be obtained from the loop current noise spectra if the relation between the loop current and the output voltage is known. Obviously the transfer function between the two signals has the dimension of an impedance called here *Transfer impedance* Z_t. It can be proved that this transfer function should always be considered as the sum of the resonator series impedance Z_q and a more or less involved transimpedance Z_c which can be obtained by using the same processes as the dipolar impedance and possibly linearized in the vicinity of the steady state:

$$v = Z_t \cdot x \qquad Z_t = Z_q + Z_c \tag{30}$$

In the particular case of the transconductance oscillator represented in Fig. 3, Z_c is merely the impedance of the input capacitance C_1 so that, in the vicinity of the oscillation frequency, the transfer impedance can be written:

$$Z_t = R_q + jL_q\omega_q\left(\frac{2\Omega}{\omega_q} - \frac{C_q}{C_1}\right) \tag{31}$$

Output voltage v and loop current x being related by a linear relation, the usual spectrum transformation applies:

$$v = Z_t \cdot x \quad \Rightarrow \quad \underset{v}{S}(\omega) = \left|\frac{Z_t(j\omega)}{Z_0}\right|^2 \underset{x}{S}(\omega) \tag{32}$$

where Z_0 is a normalization factor.

One of the key parameters of the oscillator noise analysis can be introduced by first representing the normalized impedance of the resonator series branch. In the vicinity of the resonant frequency it is given by:

$$\left|\frac{Z_q(\Omega)}{Z_q(0)}\right|^2 = \frac{R_q^2 + \left(2L_q\Omega\right)^2}{R_q^2}. \tag{33}$$

The corresponding curve represented in dashed line in Fig. 9 has a cut off frequency Ω_q which is half the bandwidth of the unloaded resonator admittance related to the resonator unloaded Q-factor by the well known relation:

$$\Omega_q = \frac{R_q}{2L_q} \quad \Rightarrow \quad Q_q = \frac{\omega_q}{2\Omega_q} = \frac{L_q\omega_q}{R_q} \tag{34}$$

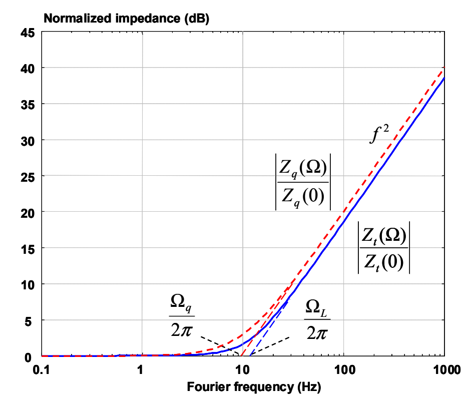

Figure 9. Normalized unloaded resonator and transfer impedances.

The normalized transfer impedance, written as:

$$\left|\frac{Z_t(\Omega)}{Z_t(0)}\right|^2 = \frac{R_q^2 + \left(2L_q\Omega - Z_1\right)^2}{R_q^2 + Z_1^2} \approx 1 + \frac{\Omega^2}{\Omega_L^2}, \tag{35}$$

represented in solid line on the same graph, has a cut-off frequency which is nothing else the Leeson's cut-off frequency straight related to the oscillator loaded Q-factor:

$$\Omega_L = \frac{\sqrt{R_q^2 + Z_1^2}}{2L_q} \quad \Rightarrow \quad Q_L = \frac{\omega_q}{2\Omega_L} = \frac{L_q\omega_q}{\sqrt{R_q^2 + Z_1^2}} \tag{36}$$

X. Noise Spectra of the Output Voltage

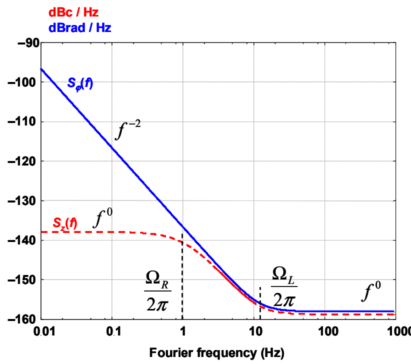

Figure 10. Additive noise spectra of the output voltage.

Applying the conversion relation (32) to the transconductance oscillator leads to the popular output voltage phase noise spectrum characterized by the Leeson's cut-off frequency as shown in Fig. 10 (solid line). Likewise, the output voltage amplitude noise spectrum has the shape shown in dashed line, characterized by the Leeson's cut-off frequency Ω_L and the closed loop half bandwidth frequency Ω_R. Another popular feature can also be evidenced by this model: the asymptotic phase noise floor that takes the simple form:

$$S_\varphi(\Omega >> \Omega_L) = 10\log\left(\frac{\hat{x}_n^2}{2y_0^2}\right) \quad (37)$$

formally demonstrates the well known fact that the noise floor decreases as the resonator drive level increases.

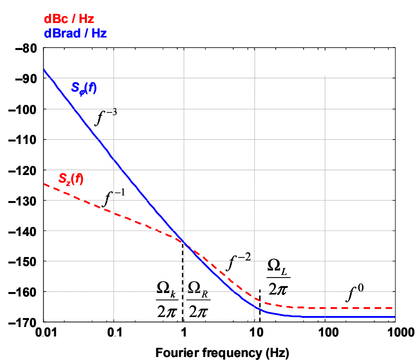

Figure 11. Parametric noise spectra of the output voltage.

Applying the same processes to the parametric noise spectra leads to the curves shown in Fig. 11 where the phase noise (solid line) exhibits a –30dB/dec slope below the corner frequency, a –20dB/dec slope between Ω_K and Ω_L and a flat noise floor above Ω_L. The amplitude noise spectrum has then the shape in dashed line in Fig. 11 where the relevant frequencies are indicated.

The asymptotic phase spectrum given by the relation:

$$S_\varphi(\Omega >> \Omega_L) = 10\log\left(\frac{\alpha_0^2 Z_1^2}{8(R_q^2 + Z_1^2)}\right) \quad (38)$$

confirms that the parametric phase noise floor doesn't depend on the resonator drive level.

When several independent noise sources are involved, the resulting noise spectrum is obtained by adding the individual noise spectra. Combining the contribution of the additive phase noise spectrum of the output voltage with the parametric phase noise spectrum, leads to the resulting phase noise shown in Fig. 12. Obviously, the resulting shape depends on the $1/f$ corner frequency and on the relative level of the individual contributions as shown in comparing Fig. 12 (a) where $\Omega_K < \Omega_L$ and Fig. 12 (b) where $\Omega_K > \Omega_L$.

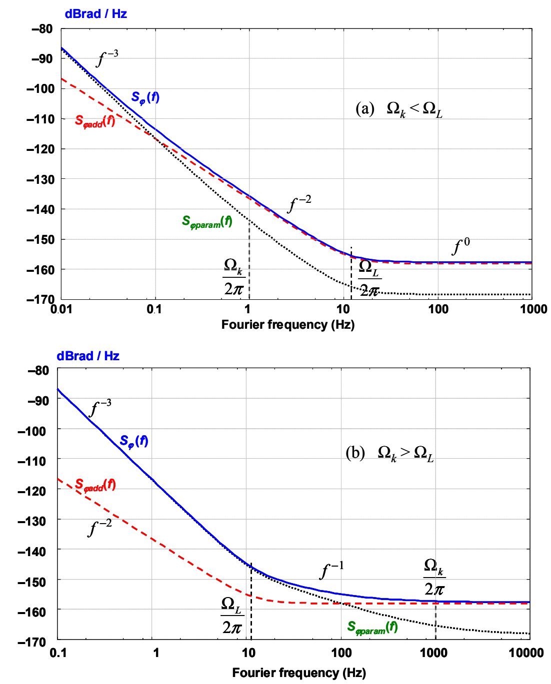

Figure 12. Additive and parametric noise spectra of the output voltage.

The analysis of the parametric noise of the resonator leads to the same result as obtained for the input capacitance parametric noise, thus it is not possible to discriminate their respective contributions.

XI. Conclusion

The dipolar model and asymptotic method turn out to be powerful tools to efficiently analyze high Q-factor circuits like quartz oscillator as they give quickly and accurately most of the relevant feature of the oscillator characteristics such as start up condition, steady state, transient and noise spectra.

It is in fact a general approach the scope of which really goes beyond the limited area of the quartz oscillator analysis.

References

[1] K. Kurokawa, "Some basic characteristics of broadband negative resistance oscillator circuits", Bell Syst. Tech. J., pp. 1937–1955, July–August 1969.

[2] E.A. Vittoz, "Quartz oscillators for watches", in Proc. of the 10th Int. Congress of Chronometry, Geneva, 1979, pp. 131–140.

[3] M. Addouche, R. Brendel, D. Gillet, N. Ratier, F. Lardet-Vieudrin and J. Delporte, "Modeling of quartz crystal oscillator by using nonlinear dipolar method", IEEE Trans. UFFC, pp. 487–495, May 3003.

[4] N. Kryloff and N.N. Bogoliuboff, Introduction to Nonlinear Mechanics, Princeton University Press, 1943.